Lovastatin-induced cholesterol depletion affects both apical sorting and endocytosis of aquaporin-2 in renal cells

G. Procino, C. Barbieri, M. Carmosino, F. Rizzo, G. Valenti and M. Svelto

Am J Physiol Renal Physiol 298:F266-F278, 2010. First published 18 November 2009;
doi: 10.1152/ajprenal.00359.2009

Am J Physiol Renal Physiol 298: F266–F278, 2010.
First published November 18, 2009; doi:10.1152/ajprenal.00359.2009.

Lovastatin-induced cholesterol depletion affects both apical sorting and endocytosis of aquaporin-2 in renal cells

G. Procino,[1]* C. Barbieri,[1]* M. Carmosino,[2] F. Rizzo,[1] G. Valenti,[1] and M. Svelto[1]

[1]*Department of General and Environmental Physiology, University of Bari, Bari, Italy; and* [2]*Department of Cell and Molecular Physiology, Yale Medical School, New Haven, Connecticut*

Submitted 25 June 2009; accepted in final form 16 November 2009

Procino G, Barbieri C, Carmosino M, Rizzo F, Valenti G, Svelto M. Lovastatin-induced cholesterol depletion affects both apical sorting and endocytosis of aquaporin-2 in renal cells. *Am J Physiol Renal Physiol* 298: F266–F278, 2010. First published November 18, 2009; doi:10.1152/ajprenal.00359.2009.—Vasopressin causes the redistribution of the water channel aquaporin-2 (AQP2) from cytoplasmic storage vesicles to the apical plasma membrane of collecting duct principal cells, leading to urine concentration. The molecular mechanisms regulating the selective apical sorting of AQP2 are only partially uncovered. In this work, we investigate whether AQP2 sorting/trafficking is regulated by its association with membrane rafts. In both MCD4 cells and rat kidney, AQP2 preferentially associated with Lubrol WX-insoluble membranes regardless of its presence in the storage compartment or at the apical membrane. Block-and-release experiments indicate that *1*) AQP2 associates with detergent-resistant membranes early in the biosynthetic pathway; *2*) strong cholesterol depletion delays the exit of AQP2 from the *trans*-Golgi network. Interestingly, mild cholesterol depletion promoted a dramatic accumulation of AQP2 at the apical plasma membrane in MCD4 cells in the absence of forskolin stimulation. An internalization assay showed that AQP2 endocytosis was clearly reduced under this experimental condition. Taken together, these data suggest that association with membrane rafts may regulate both AQP2 apical sorting and endocytosis.

membrane rafts

AQP2 IS THE WATER CHANNEL expressed in the principal cells of the collecting duct (38, 59, 67, 68, 71). Under resting conditions, AQP2 is found primarily in intracellular vesicles beneath the apical membrane. During hypovolemia or hypernatremia, in response to arginine vasopressin (AVP) binding to the V2 receptor (V2R) at the basolateral membrane, AQP2 is phosphorylated by PKA at ser256, a crucial event for the exocytosis of AQP2-bearing vesicles at the apical plasma membrane (19). AQP2 redistribution to the apical membrane has been closely correlated with a dramatic increase in membrane water permeability of the collecting duct and is responsible for the facultative water reabsorption in the collecting duct. Withdrawal of AVP triggers the endocytosis of AQP2-containing vesicles and restores the water-impermeable state of the apical membrane.

Impairment of AQP2 trafficking, produced by mutations of either V2R or AQP2 genes, is responsible for a dramatic clinical phenotype known as nephrogenic diabetes insipidus (NDI), a disease whose etiology is renal resistance to AVP and whose clinical hallmark is excretion of large volumes of dilute urine (3, 4, 13, 57).

* G. Procino and C. Barbieri contributed equally to this work.

Address for reprint requests and other correspondence: G. Procino, Dept. of General and Environmental Physiology, Univ. of Bari, Via Amendola 165/A, 70126 Bari, Italy (e-mail: g.procino@biologia.uniba.it).

At present, knowledge of the signals and the sorters responsible for AQP2 apical targeting in the collecting duct is far from complete. Apical sorting signals are less well defined than basolateral, and they can reside in either the luminal domain or membrane anchor of the targeted protein (54).

It has been shown that the proximal region of the COOH terminus of AQP2 is of importance for sorting of AQP2 to the apical membrane (14) and that both the NH_2 and COOH termini of AQP2 are essential and sufficient for sorting to forskolin (FK)-sensitive storage vesicles in AQP2-transfected Madin-Darby canine kidney (MDCK) cells (72).

AQP2 exists as a glycosylated tetramer in the membrane although it has been shown that glycosylation is neither essential for tetramerization nor for transport from the endoplasmic reticulum to the Golgi complex. Instead, the N-linked glycan is important for exit from the Golgi complex and for the sorting of AQP2 to the plasma membrane (23). In addition, the sixth transmembrane domain of AQP2, including a dileucine motif, is involved in the regulated trafficking of this water channel (76). More recently, a novel mechanism, involving a reciprocal interaction with G-actin and tropomyosin 5b, has been proposed to explain AQP2 apical trafficking (41).

If little is known about signals involved in AQP2 apical sorting, nothing is known about the sorters that can "interpret" those AQP2 intrinsic signals and drive its insertion into apical transport vesicles. The cellular components that recognize and interact with apical sorting signals have not been identified and are likely to be as diverse as the signals themselves. Among them, a clear role has been proposed for lectins, lipid rafts, and coats (37).

Transmembrane lectins, for example, are thought to recognize the sugar group of many glycoproteins and mediate their sorting into forming apical transport vesicles. At the *trans*-Golgi network (TGN), such lectins may then be funneled into apical transport vesicles by interactions between their transmembrane domains and subdomains of the membrane lipid bilayer, known as rafts, which are enriched with cholesterol and sphingolipids. Although there is evidence that raft association is not sufficient to ensure apical sorting, the raft mechanism is currently the most favored apical sorting mechanism (2).

The lipid raft hypothesis postulates that many proteins are sorted apically because they have an affinity for microdomains of glycosphingolipids and cholesterol (lipid rafts) that are assembled in the Golgi complex. According to this hypothesis, lipid rafts and their associated proteins form sorting platforms that become incorporated into apical transport intermediates that deliver them to the apical membrane.

Several lines of evidence suggest a possible association of AQP2 with membrane rafts in renal cells. *1*) By performing a proteomic analysis, Yu et al. (77) has shown that AQP2 is

associated with detergent-resistant membranes (DRMs) from rat renal collecting duct. *2*) AQP2 is enriched in the microvilli of kidney principal cells (39, 75), in MCD4 cells (unpublished observations), as in many other cell lines. It has long been recognized that the microvillar surface is organized in cholesterol/sphingolipid-enriched membrane microdomains commonly known as lipid rafts (12, 47). Moreover the role of cholesterol in AQP2 trafficking has been demonstrated by works indicating that treatment with the cholesterol-sequestering agent mβCD accumulated AQP2 at the apical plasma membrane in both isolated kidney tubules and cultured renal cells (34, 56).

A common biochemical method to analyze raft organization in biological membranes is extraction with mild detergents. Although detergent treatment disrupts most lipid-lipid interactions, a minor fraction of cell membranes is preserved and can be isolated as DRMs.

In this work, we analyzed the detergent solubility feature of AQP2 in the MCD4 mouse cortical collecting duct cell line as well as in rat kidney medulla, and we show that AQP2 preferentially associated with Lubrol-resistant membrane rafts. In addition, we demonstrated for the first time the physiological role of this association in the trafficking of AQP2.

MATERIALS AND METHODS

Antibodies and reagents. Antibodies against the transferrin receptor (TfR), flotillin-2, AQP4, and calnexin were purchased from Santa Cruz Biotechnology (www.scbt.com). Antibodies against the calcium-sensing receptor (CaSR) were from Chemicon. Antibodies against TGN46 were from Abcam; anti-Na-K-ATPase was from Upstate. An affinity-purified rabbit polyclonal antibody against human AQP2 was prepared as described elsewhere (69). EZ-link Sulfo NHS-SS-biotin and an Immunopure Immobilized Streptavidin bead suspension was purchased from Pierce (www.piercenet.com). Indomethacin, lovastatin, mevalonate, brefeldin A, p58K antibody, Optiprep, and Triton X-100 (TX-100) were from Sigma (www.sigmaaldrich.com). Lubrol-WX (L-WX) was purchased from Serva (www.serva.de). LDL-depleted serum was prepared from FBS by density centrifugations (46).

Cell culture, transfection, and animals. Mouse cortical collecting duct MCD4 cells, stably expressing human AQP2, were generated as described elsewhere (28).

Mouse cortical collecting duct M-1 cells (16), originating from mice transgenic for the early region of simian virus 40, were purchased from the European Collection of Cell Cultures and cultured in DMEM/F12, 1:1, supplemented with 5% fetal bovine serum, 2 mM L-glutamine, 100 IU/ml penicillin, 100 μg/ml streptomycin, and 5 μM dexamethasone. For transfection, cells were grown until ~95% confluent and then transfected with a plasmid encoding VSV-tagged rat AQP4 (35). Lipofectamine 2000 (Invitrogen; www.invitrogen.com) was used for transfections according to the manufacturer's instructions.

Selection of the positive clones was made with geneticin (500 μg/ml, GIBCO; www.invitrogen.com) for 10–15 days. Resistant clones were isolated; AQP4 expression and localization were evaluated by Western blotting and immunofluorescence. One of these clones, referred to as M1-AQP4, was used in subsequent studies.

To reduce cholesterol levels, 24 h after plating cells were treated with 4 μM lovastatin and 250 μM mevalonate for 3 days in complete medium (mild cholesterol depletion) or in LDL-depleted medium (strong cholesterol depletion).

Block and release experiments were performed as follows. MCD4 and M1-AQP4 were treated overnight (16 h) with brefeldin A (BFA; 1 μg/ml) in the culture medium. The day after, BFA was washed out and cells were analyzed at different time points: 0, 30 min, 1 h 30 min, 3 h, and 4 h 30 min.

In all experiments, MCD4 cells were treated with indomethacin (5×10^{-5} M) overnight in the culture medium to reduce the basal cAMP concentration. Stimulation was performed with 10^{-4} M FK in the culture medium for 20 min.

Wistar-Kyoto rats (200–250 g) from Harlan (www.harlan.com) were used for the experiments. The animals were divided into two groups: the control group ($n = 6$) had free access to water (control), and a second group was thirsted for 18 h ($n = 6$; water restricted). All animal experiments carried out were approved by the Institutional Committee on Research Animal Care, in accordance with the Italian Institute of Health Guide for the Care and Use of Laboratory Animals.

Detergent solubility assay. Whole MCD4 cells or purified plasma membranes were resuspended in ice-cold lysis buffer (150 mM or 1 M NaCl, 2 mM EGTA, 50 mM Tris · HCl, 1 mM PMSF, protease inhibitor cocktail, pH 7.5) containing 1% TX-100 or 1% L-WX and incubated for 30 min at 4°C. Cell lysates were centrifuged at 4°C for 1 h at 100,000 *g*. The soluble (supernatant) and insoluble (pellet) fractions (5 μg of total proteins) were analyzed by SDS-PAGE followed by immunoblotting (see below).

Cell and tissue fractionation. MCD4 cells (resting or FK-stimulated) were resuspended in homogenizing buffer (300 mM sucrose, 25 mM imidazole, 1 mM EDTA, 1 mM PMSF, protease inhibitor cocktail, pH 7.2) and homogenized with five strokes in a Potter-Elvehjem at 1,250 rpm. The homogenate was spun at 4,000 *g* for 15 min, and the pellet was discarded. The supernatant was spun at 17,000 *g* for 30 min to obtain a pellet enriched with plasma membrane.

The same protocol was used to isolate plasma membrane from kidney inner medulla of control and water-restricted rats.

Fractionation of MCD4 homogenate on Optiprep was performed as follows. MCD4 cells were resuspended in 0.25 M sucrose, 1 mM EDTA, 10 mM HEPES-NaOH, pH 7.4, and homogenized by Dounce homogenization and repeated passages through a fine syringe needle. A postnuclear supernatant fraction (1,500 *g*, 10 min) was collected and separated by centrifugation using an Optima TLX ultracentrifuge (Beckman) with a swinging bucket rotor (SW40) at 200,000 *g* for 2.5 h in a 2.5–30% continuous gradient of OptiPrep (1 ml of 2.5%, 2 ml each of 5, 7.5, and 10%, 0.5 ml of 12.5%, 2 ml of 15%, and 0.5 ml each of 17.5, 20, and 30%). Twenty-four fractions of 500 μl were collected from top to bottom, and proteins were subjected to SDS-PAGE. For immunoblotting, the following antibodies were used: CaSR (apical membrane), p58K (Golgi), TGN38 (TGN), calnexin (RER), and AQP2. *Fractions 19–23*, referred to as endoplasmic reticulum (ER) fractions, and *fractions 12–16*, referred to as TGN fractions, were pooled (100 μl of each fraction), and membranes were sedimented at 100, 000 *g* for 1 h. Membranes were subjected to a detergent solubility assay as described. *Fractions 16* and *21*, displaying the higher content of AQP2 among TGN ad ER fractions, respectively, were also analyzed alone.

Floatation assay on discontinuous sucrose gradient. Whole cells or plasma membrane fractions from both MCD4 cells and kidney papilla were resuspended in MBS buffer (25 mM MES and 150 mM NaCl, 1 mM PMSF, protease cocktail inhibitor, pH 6.5) containing 1% TX-100 or L-WX and incubated for 30 min on ice. Lysates were mixed with an equal volume of MBS+90% sucrose and laid at the bottom of an ultracentrifuge tube. Then, the same volumes of MBS+30% sucrose and MBS+5% sucrose were gently overlaid on top of the samples, and the gradients were centrifuged at 200,000 *g* for 18 h at 4°C. Depending on the experiments, 8 or 12 fractions of equal volume were collected from top to bottom of the tube. Ten microliters of each fraction were separated on NuPage gel and assessed by Western blotting for the presence of AQP2, AQP4, flotillin-2, and TfR.

Cholesterol assay. MCD4 cells were cultured for 72 h with lovastatin and mevalonate in control medium (mild cholesterol depletion) or in LDL-depleted medium (strong cholesterol depletion). Cell lysates were assayed for cholesterol content using an Olympus enzy-

matic color test (catalog no. OSR6x16, www.olympus.com) according to the manufacturer's instructions.

Apical surface biotinylation and biochemical internalization assay. Both control and cholesterol-depleted cells were grown on 0.4-μm cell culture inserts and incubated in the presence or in the absence of 10^{-4} M FK for 20 min in the culture medium at 37°C. Apical surface biotinylation and endocytosis assays were performed as described previously (30, 49). Briefly, filters were rapidly washed in ice-cold Earle's balanced salt solution (EBS) buffer for biotinylation, and the apical side was incubated with biotin (2.5 mg/ml in EBS buffer) on ice for 30 min. Unbound biotin was quenched by 10-min incubation in quenching buffer on ice. For biotinylation experiments, cells were scraped in lysis buffer, sonicated, and incubated at 37°C for 20 min. For internalization experiments, surface proteins were permitted to become internalized by warming the cells to 37°C for 0, 10, 20, 40, and 60 min. Next, cells were washed with ice-cold PBS with $CaCl_2$ and $MgCl_2$ (PBS-CM) and treated for 3 × 15 min with ice-cold 100 mM sodium 2-mercaptoethane sulfonate (MesNa) in 100 mM NaCl, 1 mM EDTA, 50 mM Tris (pH 8.6), and 0.2% BSA. The cell-impermeable MesNa removes cell surface-bound biotin, while internalized biotinylated proteins are protected. Excess MesNa was quenched with ice-cold 120 mM iodoacetic acid in PBS-CM, and cells were lysed as described above for cell surface biotinylation. Lysates were sonicated for 30 s, incubated at 37°C for 20 min, and unsolubilized material was pelleted at 13,000 *g* for 10 min. Biotinylated proteins were precipitated with a streptavidin bead suspension under rotation at 4°C overnight. Beads were washed and biotinylated proteins were extracted in NuPAGE LDS sample buffer with 100 mM DTT, heated at 95°C for 10 min, and resolved on NuPAGE gels.

Gel electrophoresis and immunoblotting. Cellular proteins (lysates, sucrose gradient fractions, and biotinylated proteins) were separated on 4–12% NuPAGE Bis-Tris gels (www.invitrogen.com) under reducing conditions. Protein bands were electrophoretically transferred to ImmobilonP membranes (www.millipore.com) for Western blot analysis, blocked in TBS-Tween containing 3% BSA, and incubated with primary antibodies. Immunoreactive bands were detected with secondary antibody conjugated to horseradish peroxidase. After each step, the membranes were washed with TBS-Tween. Membranes were developed with SuperSignal West Pico Chemiluminescent Substrate (www.piercenet.com) and exposed to autoradiographic Kodak Biomax XAR film (www.sigma-aldrich.com). Band intensities were quantitated by densitometric analysis using National Institutes of Health ImageJ software. *P* values were calculated by Student's *t*-test for unpaired data.

Immunofluorescence. MCD4 or M1-AQP4 cells were fixed with 4% PFA for 15 min. After two washes, cells were permeabilized with 0,1% NP-40 for 5 min. Both fixation and permeabilization were performed at 4°C in PBS. Cells were blocked in 1% BSA in PBS (saturation buffer) for 30 min at RT, followed by incubation with affinity-purified antibody against AQP2 (1:1,000) or AQP4 (1:500) for 1 h at 37°C in saturation buffer. Bound antibodies were detected with Alexa Fluor-conjugated donkey anti-rabbit or anti-goat IgG antibody, 1:1,000, for 1 h at room temperature. All incubations were performed from both sides of the filters. Washed filters were mounted on microscope glasses, and confocal images were obtained with a laser-scanning fluorescence microscope (Leica TSC-SP2).

RESULTS

AQP2 preferentially associates with Lubrol DRMs. To analyze the possible association of AQP2 with lipid rafts, we first checked the solubility of AQP2 in different nonionic detergents. For this, we used a mouse collecting duct cell line stably transfected with human AQP2, MDC4 cells, previously characterized in our laboratory (28, 49). As detergents, we used TX-100, conventionally used to isolate membrane rafts, and L-WX, another nonionic detergent with a higher hydrophilic-lipophilic balance than Triton X-100.

We first investigated whether AQP2 is associated with DRMs by a detergent solubility assay. Briefly, MCD4 cells were lysed in 1% TX-100 or 1% L-WX at 4°C. Lysates were then fractionated into supernatant (soluble fraction) and pellet (insoluble fraction), and equal amounts of total proteins analyzed by SDS-PAGE followed by immunoblotting for AQP2.

When solubilized in TX-100, AQP2 was almost equally distributed between soluble and insoluble fractions (Fig. 1*A*). Interestingly, AQP2 was completely insoluble in L-WX (Fig. 1*A*).

To demonstrate the presence of membrane rafts in the insoluble fraction obtained after ultracentrifugation, the same samples were assayed for the presence of flotillin-2, a marker of membrane raft domains, and TfR, a protein not associated with membrane rafts. Regardless of the detergent used, flotillin-2 and TfR were exclusively associated with insoluble and soluble fractions, respectively, indicating that this experimental procedure can effectively separate membrane rafts vs. nonrafts.

Detergent insolubility of a membrane protein can result from its association with DRM rafts and/or anchoring to cytoskeletal elements. To discriminate between these possibilities, the same experiment was repeated using buffers of high ionic strength (high NaCl), a treatment known to disrupt the cytoskeleton (17).

The proportion of AQP2 recovered in the pellet and supernatant was the same as with low-ionic-strength buffer (Fig. 1*A*), indicating that the insolubility of AQP2 in TX-100 and L-WX is not due to interaction with cytoskeletal elements.

Altogether, these observations indicate that AQP2 preferentially associates with Lubrol DRMs.

Association of AQP2 with L-WX membrane rafts is independent of AQP2 translocation to the plasma membrane. To address the question of whether AQP2 association/dissociation with membrane rafts is modulated during translocation to the apical plasma membrane, we separated raft vs. nonraft membrane from detergent extracts of resting or FK MCD4 cells on a sucrose gradient. As previously shown, in MDC4 cells AQP2 was present in an intracellular compartment and translocates to the apical plasma membrane upon stimulation with FK (49). Given the preferential association of AQP2 with Lubrol DRMs, we extracted MCD4 cells with 1% L-WX at 4°C and subjected the lysates to a floatation assay on a sucrose density gradient. In these conditions, membrane rafts will float from the bottom to the top of the sucrose gradient during centrifugation. Sequential fractions were taken from the top of the gradients and analyzed by immunoblotting to assess the distribution of AQP2 between raft and nonraft fractions. In all experiments, membrane raft fractions were identified as those positive for flotillin-2, whereas nonraft fractions were identified as positive for TfR.

As shown in Fig. 1*B*, when cells were extracted with 1% L-WX, most of the AQP2 was found to float to the flotillin-positive, low-density fractions of the gradient. FK did not induce any further association of AQP2 with L-WX-insoluble microdomains, indicating that AQP2 is already associated with Lubrol rafts in the storage compartment rather than associating with them upon fusion with the plasma membrane. The cholesterol content of each fraction was measured with a colorimetric method and reported in Fig. 1*B*, indicating that AQP2 floated, along with cholesterol, to the same region of the gradient. MCD4 cells were also subjected to the same protocol,

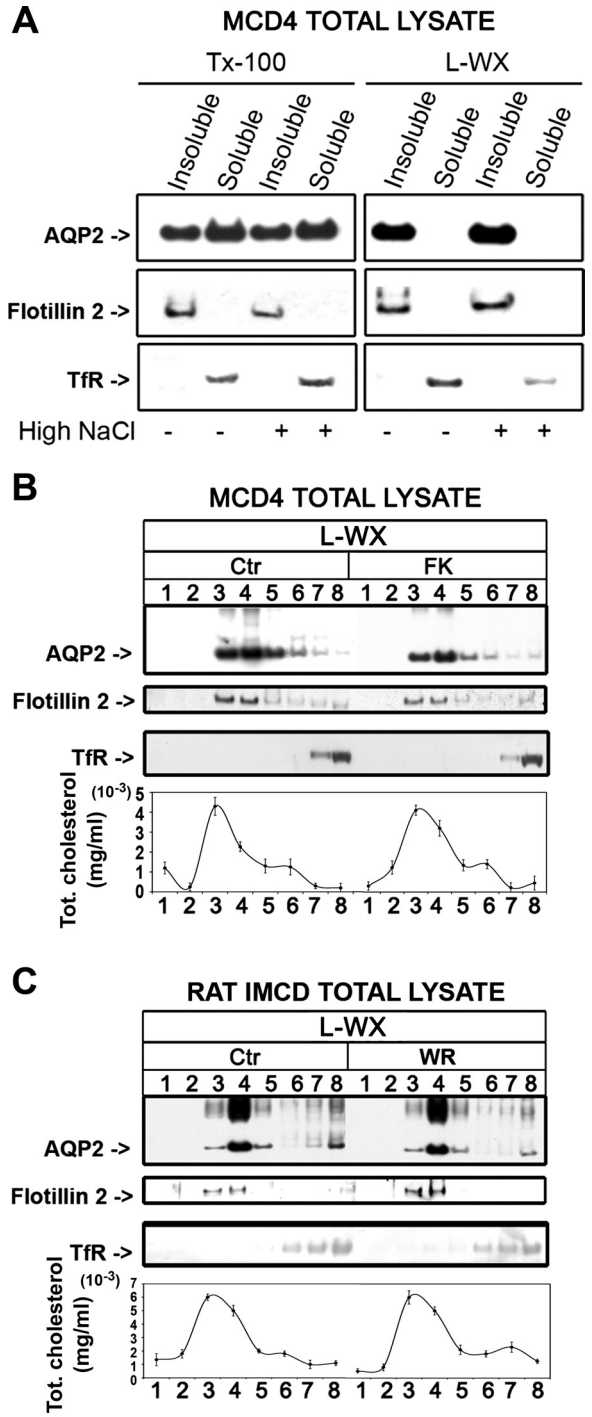

Fig. 1. Aquaporin-2 (AQP2) insolubility in Lubrol WX (L-WX) reflects its association with detergent-resistant complexes. *A*: resting or forskolin (FK)-stimulated MCD4 cells were lysed in 1% Triton X-100 (TX-100) or L-WX at 4°C in the presence or in the absence of 1 M NaCl and centrifuged for 1 h at 100,000 *g*. Supernatant (soluble) and pellet (insoluble) were analyzed by SDS-PAGE followed by immunoblotting for AQP2, flotillin-2, and transferrin receptor (TfR). *B*: resting or FK-stimulated MCD4 cells were lysed in L-WX at 4°C and subjected to flotation on a sucrose density step gradient. The gradient fractions (8 from *top* to *bottom* of the tubes) were analyzed by SDS-PAGE followed by immunoblotting for AQP2, flotillin-2, and TfR. Total cholesterol content of each fraction was measured and reported as a diagram. Values are means ± SE of 3 independent measurements. *C*: kidney papillae from control and water-restricted (WR) rats were subjected to flotation on a sucrose density step gradient as described above. IMCD, inner medullary collecting duct. All pictures are representative of at least 3 experiments with comparable results.

after solubilization in TX-100 instead of L-WX. These results confirmed a partial association of AQP2 with TX-100-resistant DRMs (data not shown).

The association of AQP2 with L-WX-resistant microdomains observed in MCD4 cells was also confirmed in native kidney tissue. Raft vs. nonraft membranes were separated on a discontinuous sucrose gradient using, as starting material, a L-WX lysate of inner medulla of control vs. water-restricted rats. It is known that water restriction increases plasma levels of vasopressin inducing the translocation of AQP2 into the apical membrane of collecting duct principal cells. Samples from randomly chosen kidneys were analyzed in parallel by immunofluorescence to verify the different intracellular localization of AQP2 in control and water-restricted rats. AQP2 was found intracellularly expressed in control animals and accumulated at the apical plasma membrane in water-restricted animals (data not shown). AQP2 floated mainly to the flotillin-2-positive/cholesterol-enriched fractions of the gradient in both control and water-restricted animals. Water restriction did not change AQP2 distribution along the gradient (Fig. 1*C*).

These data indicate that the preferential association of AQP2 with L-WX-insoluble membrane rafts in cultured cells as well as in native kidney tissues is not modified during the physiological cascade of events that leads to AQP2 translocation to the apical plasma membrane.

To rule out the possibility that the partition of AQP2 into cholesterol-rich/flotillin-positive fractions was an artifact of the detergent extraction, a detergent-free method was used to separate different membrane domains (63). The results are reported in Supplemental Fig. S1 and show that, regardless of the presence of the detergent, AQP2 floated to the same flotillin-positive fractions.

To better analyze whether AQP2 inclusion in the membrane rafts is modulated upon AQP2 exocytosis at the plasma membrane, we next focused our attention specifically at the plasma membrane-associated AQP2. Plasma membrane-enriched fractions were isolated from resting and FK-stimulated MCD4 cells using a conventional method (36), solubilized in 1% TX-100 or L-WX, and fractionated into a pellet and supernatant upon ultracentrifugation. Interestingly, plasma membrane-associated AQP2 was completely soluble in TX-100 and fully insoluble in L-WX (Fig. 2*A*, *right*). The translocation of AQP2 to the plasma membrane was confirmed by the increased amount of membrane-associated AQP2 upon FK stimulation in the starting material (Fig. 2*A*; *left*). Plasma membranes from both resting and FK-stimulated MCD4 cells were also subjected to the flotation assay on a sucrose gradient. The small amount of plasma membrane-associated AQP2 observed in control conditions was already associated with L-WX rafts. Interestingly, after FK stimulation, AQP2 increased mainly in the membrane raft fractions, suggesting that AQP2 translocated to the apical membrane already in association with membrane rafts (Fig. 2*B*). This observation was also confirmed in rat inner medulla of control vs. water-restricted rats (Fig. 2*C*).

Basolateral AQP4 is associated with membrane rafts. Before investigating any possible role of membrane raft association in AQP2 apical sorting and trafficking, we asked the question of whether AQP2 localization in Lubrol rafts was specific for AQP2 or a common feature of other aquaporins. AQP4 is expressed on the basolateral membrane of collecting duct principal cells (70). As for many basolateral proteins,

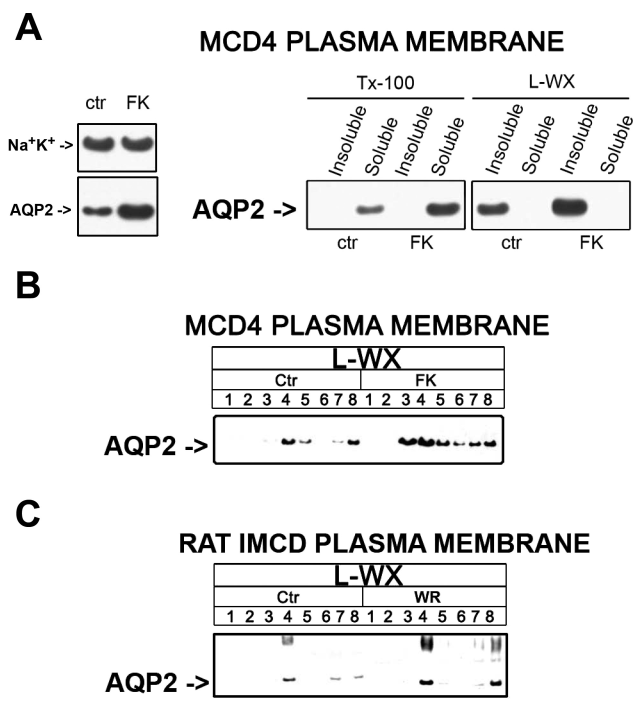

Fig. 2. Plasma membrane-expressed AQP2 is associated with Lubrol detergent-resistant complexes. *A*: plasma membrane-enriched fraction from resting or FK-stimulated MCD4 cells were lysed in 1% TX-100 or L-WX at 4°C and centrifuged for 1 h at 100,000 *g*. The supernatant (soluble) and pellet (insoluble) were analyzed by SDS-PAGE followed by immunoblotting for AQP2. *B*: plasma membrane-enriched fraction from resting or FK-stimulated MCD4 cells were lysed in L-WX at 4°C and subjected to flotation on a sucrose density step gradient. The gradient fractions (8 from *top* to *bottom* of the tubes) were analyzed by SDS-PAGE followed by immunoblotting for AQP2. *C*: plasma membrane-enriched fraction from kidney papillae of control and WR rats were subjected to flotation on a sucrose density step gradient as described above. All pictures are representative of at least 3 experiments with comparable results.

AQP4 sorting at the TGN might rely on the presence of C-terminal amino acid sequences rather than on the association with membrane rafts (35). M1-AQP4 cells were obtained by stably transfecting M-1 cells, the parental cell line used to obtain MCD4, with rat AQP4 cDNA. In this cell line, AQP4 was expressed on the basolateral membrane, as visualized by confocal scans taken in both *XY*- and *XZ*-planes (Fig. 3*A*). L-WX extracts of M1-AQP4 cells were subjected to flotation assays to assess AQP4 association with membrane rafts. Most of AQP4 floated to the raft-enriched fractions (Fig. 3*B*). The same protocol was applied to L-WX extracts from rat inner medulla, and the results confirmed the association of AQP4 with L-WX-insoluble membrane rafts in native kidney (Fig. 3*C*).

These results indicated that, although sorted to the basolateral membrane, AQP4 is associated with membrane rafts in renal cells and that L-WX insolubility is not a specific feature of AQP2.

AQP2 associates with DRMs early during its maturation. The observation that AQP2 is insoluble in L-WX already in the storage compartment, before its arrival at the apical surface, suggested an investigation into how early AQP2 associated with membrane rafts during its maturation pathway. To this end, localization and detergent insolubility of AQP2 during maturation from the ER to the storage compartment were studied in BFA-treated MCD4 cells. BFA is a fungal metabolite that inhibits the secretory pathway by blocking the anterograde vesicular transport of proteins from the ER to the Golgi complex. We have already demonstrated that AQP2 can be reversibly accumulated in the ER upon BFA treatment in CD8 renal cells. In the same work, using the pulse-chase approach, we measured the half-life of AQP2 (~8 h) and demonstrated that BFA treatment do not interfere with AQP2 turnover (50). A similar value for AQP2 half-life had been previously reported in MDCK cells (23).

Treatment of MCD4 cells with BFA, followed by BFA washout at the indicated time points (Fig. 4*A*), allowed us to follow AQP2 trafficking from the ER to the storage compartment. At each time point, AQP2 insolubility in L-WX was evaluated as an index of AQP2 association with membrane rafts (Fig. 4*A*).

In control untreated cells, AQP2 was localized in intracellular vesicles and was completely insoluble in L-WX. In cells treated for 16 h with BFA, AQP2 was accumulated in the ER (see colocalization with calnexin in Supplemental Fig. S3), and no apparent presence of AQP2 in the post-ER compartments was seen. Interestingly, although a significant fraction was recovered in the detergent-soluble fractions, most AQP2 was already L-WX insoluble, suggesting an early association of AQP2 with DMRs in the ER.

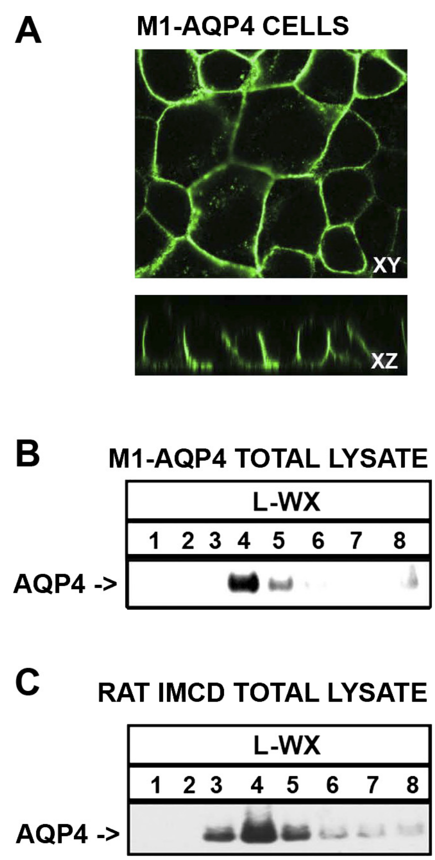

Fig. 3. AQP4 is associated with Lubrol detergent-resistant membranes. *A*: immunofluorescence confocal analysis of AQP4 expressed in M1-AQP4 cells. *B*: M1-AQP4 cells were lysed in L-WX at 4°C and subjected to flotation on a sucrose density step gradient. The gradient fractions (8 from *top* to *bottom* of the tubes) were analyzed by SDS-PAGE followed by immunoblotting for AQP4. *C*: rat kidney papillae were subjected to flotation on a sucrose density step gradient as described above. All pictures are representative of at least 3 experiments with comparable results.

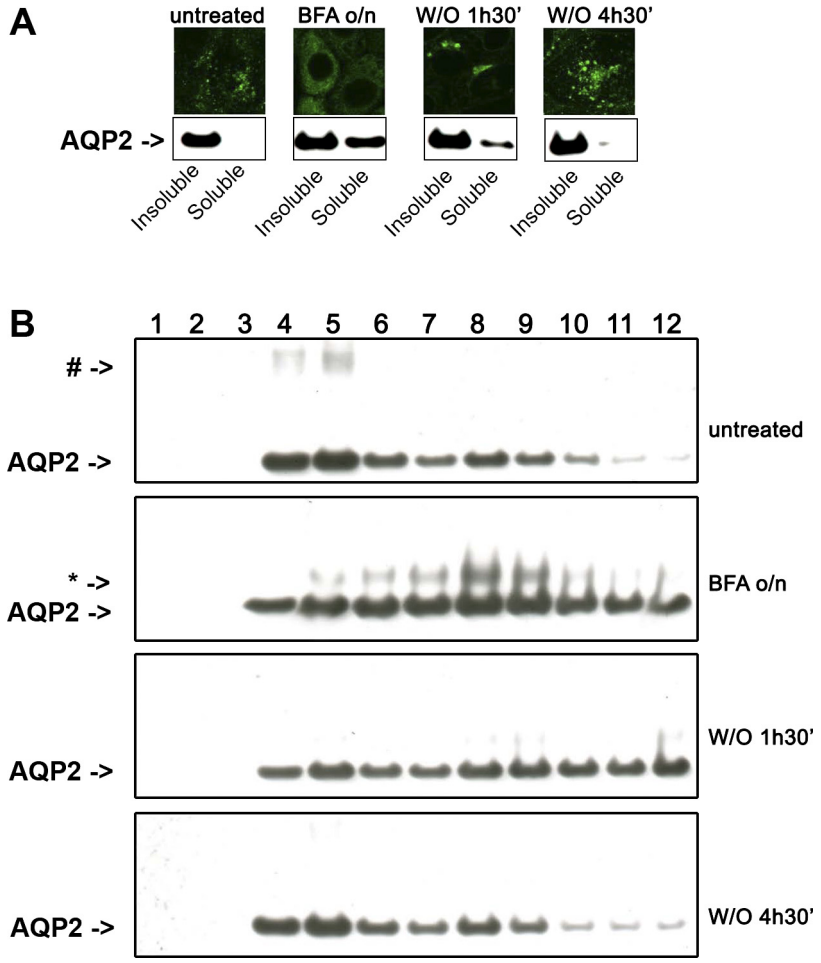

Fig. 4. Block-and-release experiments showing that AQP2 associates with Lubrol detergent-resistant membranes early in the secretory pathway. *A*: at each step of block-and-release experiment (see MATERIALS AND METHODS), AQP2 expression was analyzed by either immunofluorescence confocal analysis (*top*) or detergent solubility assay (*bottom*). WO, washout. *B*: at each step of block-and-release experiment, MCD4 cells were lysed at 4°C in Lubrol-WX and subjected to flotation on a sucrose density step gradient. The gradient fractions (12 from *top* to *bottom* of the tubes) were analyzed by SDS-PAGE followed by immunoblotting for AQP2. #, Mature AQP2 glycosylated band; *, high-mannose AQP2 glycosylated band; BFA, brefeldin A. All pictures are representative of at least 3 independent experiments.

After 1 h 30 min of BFA washout, AQP2 staining was accumulated in the Golgi complex, as indicated by colocalization experiments with the Golgi marker p58K protein (Supplemental Fig. S3). At this time point, AQP2 acquired the full Lubrol insolubility consistent with the association with membrane rafts in the Golgi apparatus.

After 4 h 30 min of BFA washout, the pattern of AQP2 localization was similar to that found in control conditions, displaying most of the AQP2 localized in cytoplasmic vesicles and completely insoluble in L-WX (Fig. 4*A*)

MCD4 cells were also subjected to the floatation assay under these experimental conditions. As shown in Fig. 4*B*, in untreated cells AQP2 floated to the lighter fractions of the gradient (*fractions 4–9*), with the greatest enrichment in flotillin-positive *fractions 4* and *5* (data not shown). When AQP2 was accumulated in the ER by BFA treatment, its distribution along the gradient was strongly affected. In addition to the 29-kDa unglycosylated band, the presence of the 32-kDa glycosylated high-mannose band (* in Fig. 4*B*), instead of the mature 35- to 45-kDa glycosylated band (# in Fig. 4*B*), confirmed that AQP2 was accumulated in the ER and no appreciable amount of AQP2 was present in post-ER compartments. Compared with untreated cells, a small but significant amount of AQP2 shifted toward the heavier fractions of the gradient (*fractions 10–12*), consistent with the presence of the Lubrol-soluble AQP2 component already observed in Fig. 4*A*. Moreover, the bulk of AQP2 was shifted toward *fractions 8* and *9* rather than *fractions 4* and *5*. This might reflect the association of AQP2 in the ER with membrane raft-like domains (see DISCUSSION). One hour 30 minutes after BFA washout, when AQP2 is transiting the Golgi apparatus, the amount of AQP2 associated with *fractions 8* and *9* decreased, with a concomitant increase in AQP2 associated with *fractions 4* and *5*. This shift in AQP2 distribution along the gradient may reflect the association of AQP2 with membrane rafts in the Golgi apparatus with a consequent decrease in the buoyant density of these microdomains. Prolongation of BFA washout to 4 h 30 min resulted in AQP2 sorting to the vesicular storage compartment concomitant with a distribution of AQP2 along the gradient similar to that obtained in untreated cells.

To further investigate the association of AQP2 with DRMs in the ER, MCD4 cells were subjected to fractionation by an Optiprep step gradient to separate the ER from other intracellular membranes. Results are reported in Fig. 5. Fractions at the bottom of the gradient were positive for the ER marker calnexin and essentially devoid of significant contamination by plasma membranes, Golgi, or TGN as assessed by immunoblot analysis. A small but significant fraction of AQP2 was associated with the ER as shown by the 32-kDa glycosylated band. ER- and TGN-enriched fractions were pooled and subjected to a detergent solubility assay. The amount of ER-associated AQP2 resulted mostly insoluble in Lubrol-WX.

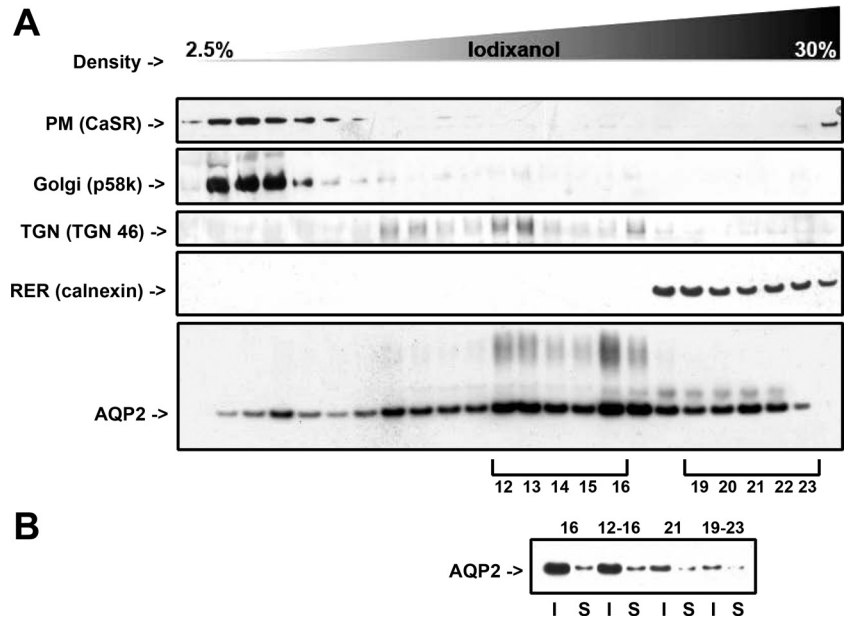

Fig. 5. Membrane fractionation. Endoplasmic reticulum (ER)-associated AQP2 is Lubrol insoluble. *A*: MCD4 homogenate was fractionated by Optiprep step gradient. Fractions were analyzed by immunoblotting for the abundance of markers of subcellular membranes: calcium-sensing receptor (CaSR; apical plasma membranes), p58K (Golgi apparatus), TGN46 [*trans*-Golgi network (TGN)], and calnexin (ER). *B*: fractions, enriched in TGN (*16* or *12–16* combined) or ER (*21* or *19–23* combined), were subjected to the detergent solubility assay and probed for AQP2 by immunoblotting. I, insoluble; S, soluble. Pictures are representative of 3 independent experiments.

Mild cholesterol depletion induced AQP2 accumulation at the apical plasma membrane in MCD4 cells by inhibiting AQP2 endocytosis. To shed light on the possible functional role of membrane raft association in the sorting/trafficking of AQP2, we next decided to deplete cellular cholesterol, a fundamental component of membrane rafts. We chose to inhibit endogenous synthesis of cholesterol by statins rather than sequestering membrane cholesterol by the commonly used the methyl-β-cyclodextrin (mβCD) method. Statins are known blockers of endogenous cholesterol synthesis because of their inhibitory effect on the enzyme 3-hydroxy-3-methylglutaryl coenzyme A reductase, which produces mevalonate, an early precursor of cholesterol. Statin treatment is a much gentler approach compared with mβCD, which routinely depletes ~60% of cellular cholesterol (31). Another important distinction is that mβCD is known to deplete cholesterol from the plasma membrane, and the depletion effect of mβCD on intracellular organelles most likely is secondary to the initial events in the plasma membrane. Statin treatment, on the other hand, would decrease cholesterol in the ER membrane initially and this effect will propagate to other cellular organelles.

MCD4 cells were grown on porous filters in complete culture medium supplemented with lovastatin. The de novo synthesis of cholesterol in the ER was inhibited by lovastatin in the presence of small amounts of mevalonate to allow the synthesis of nonsterol products, thus reducing the toxic effects due to complete cholesterol deprivation (31, 51). As reported in Table 1, lovastatin+mevalonate treatment in complete culture medium (mild cholesterol depletion) reduced the level of cellular cholesterol to ~40% compared with the control.

Confluent monolayers were then treated with or without FK, and the localization of AQP2 was analyzed by confocal microscopy.

As shown in Fig. 6*A*, in control cells, AQP2 was localized in intracellular vesicles and FK stimulation induced a complete translocation of AQP2 to the apical plasma membrane as previously described (49). Interestingly, the inhibition of de novo cholesterol synthesis produced by lovastatin treatment accumulated a large amount of AQP2 at the apical plasma membrane even in the absence of FK stimulation. FK stimulation of cholesterol-depleted cells caused an accumulation of AQP2 at the apical membrane comparable to that obtained in the absence of lovastatin.

To semiquantify this effect, cells treated as described above were subjected to apical surface biotinylation. Figure 6*B* and the relative densitometric analysis in Fig. 6*C* show the effect of cholesterol depletion on AQP2 apical accumulation in both unstimulated (control) and FK-stimulated cells.

In cells with normal cholesterol levels, FK stimulation resulted in a nearly threefold increase in biotinylated AQP2 at the apical surface compared with unstimulated cells. Cholesterol depletion per se was able to induce a comparable accumulation of AQP2 at the apical plasma membrane. FK stimulation of cholesterol-depleted cells promoted a small additional increase in apical AQP2.

Cholesterol has been suggested to play a role in protein endocytosis at the plasma membrane (1, 53, 65). Therefore, we next investigated whether the lovastatin-induced AQP2 accumulation at the plasma membrane was due to the inhibition of AQP2 endocytosis. To this end, we performed an internalization assay for AQP2 on MCD4 cells in the control condition or after mild cholesterol depletion. Cells were stimulated with FK for 20 min, biotinylated on the apical side with cleavable

Table 1. *Effect of mild or strong cholesterol depletion on total cholesterol concentration in MCD4 cells*

Sample	Total Cholesterol, mg/dl	% of Reduction,
Control	8.54 ± 0.05	
Mild cholesterol depletion	5.27 ± 0.08	8.26 ± 0.95*
Strong cholesterol depletion	3.51 ± 0.07	58.9 ± 0.91*

Values are means ± SE; $n = 3$. MCD4 cells were cultured for 72 h with lovastatin and mevalonate in control medium (mild cholesterol depletion) or in LDL-depleted medium (strong cholesterol depletion). Total cholesterol was measured in cell lysates as described in MATERIALS AND METHODS. *P 0,0001 vs. control.

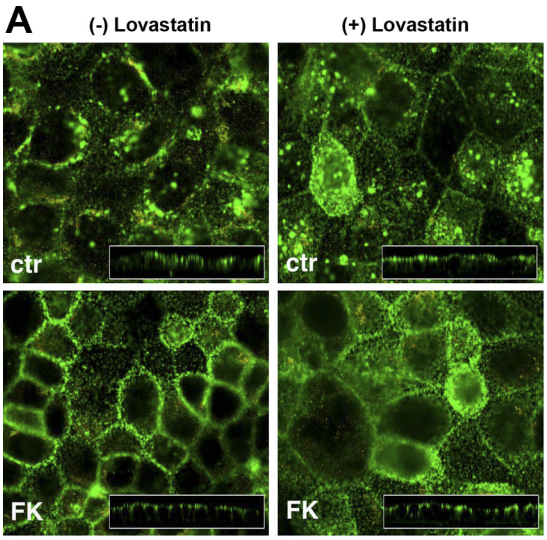

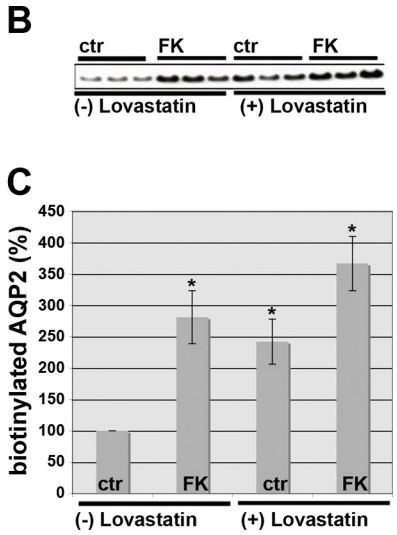

Fig. 6. Mild cholesterol depletion accumulates AQP2 at the plasma membrane. *A*: resting (control; ctr) and FK-stimulated (FK) MDC4 cells were analyzed for AQP2 immunolocalization under a normal level of cholesterol (−lovastatin) and after mild cholesterol depletion (+lovastatin). *B*: MDC4 cells, treated in the same experimental conditions described above, were subjected to apical surface biotinylation experiments. Biotinylated proteins were recovered and immunoblotted for AQP2. *C*: densitometric analysis of 29-kDa biotinylated AQP2 band. Values are means ± SE of 3 independent experiments. The amount of biotinylated AQP2 obtained in resting cells under a normal level of cholesterol (ctr, −lovastatin) was set as 100%. $*P < 0.05$ relative to ctr, −lovastatin.

biotin, returned to 37°C to allow internalization, then were treated with the membrane-impermeant reducing agent MesNa.

Internalized AQP2 was protected from cleavage and thus recovered by immobilized streptavidin. As shown in Fig. 7, more AQP2 was protected from MesNa cleavage at each successive time point (10–60 min) in control MCD4 cells compared with cholesterol-depleted cells. These data suggest that membrane cholesterol is required for internalization of AQP2 in MCD4 cells and may explain the lovastatin-induced accumulation of AQP2 at the apical plasma membrane.

Strong cholesterol depletion affects AQP2 but not AQP4 sorting at the Golgi apparatus in renal cells. In a few cells, besides apical membrane accumulation of AQP2, mild cholesterol depletion induced AQP2 localization in large vesicular structures in a perinuclear region. This observation could indicate an impairment of AQP2 sorting under reduced cholesterol levels. To further investigate this possibility, we induced a stronger depletion of intracellular cholesterol levels by culturing cells in LDL-deficient medium before treatment with lovastatin. Under this condition, cells can only rely on de novo synthesis of cholesterol to sustain cell growth and lovastatin can produce stronger cholesterol depletion (52). As reported in Table 1, treatment with lovastatin+mevalonate in LDL-depleted culture medium (strong cholesterol depletion) reduced the level of endogenous cholesterol to ~60% compared with the control.

Interestingly, in MCD4 cells, strong cholesterol depletion produced a clear accumulation of AQP2 in a perinuclear region strictly associated with the Golgi apparatus. Supplemental Fig. S3 shows the AQP2 (green) and peripheral Golgi protein 58K (red) staining in MCD4 cells subjected to strong cholesterol depletion for 72 h. A consistent amount of AQP2 is expressed in large vesicular structures that are positive for the Golgi marker 58K protein. This likely indicates an accumulation of AQP2 at the Golgi sorting station upon cholesterol depletion.

To investigate the possible role of cholesterol in AQP2 sorting/trafficking, MCD4 and M1-AQP4 cells, expressing AQP2 and AQP4, respectively, were subjected to the block-

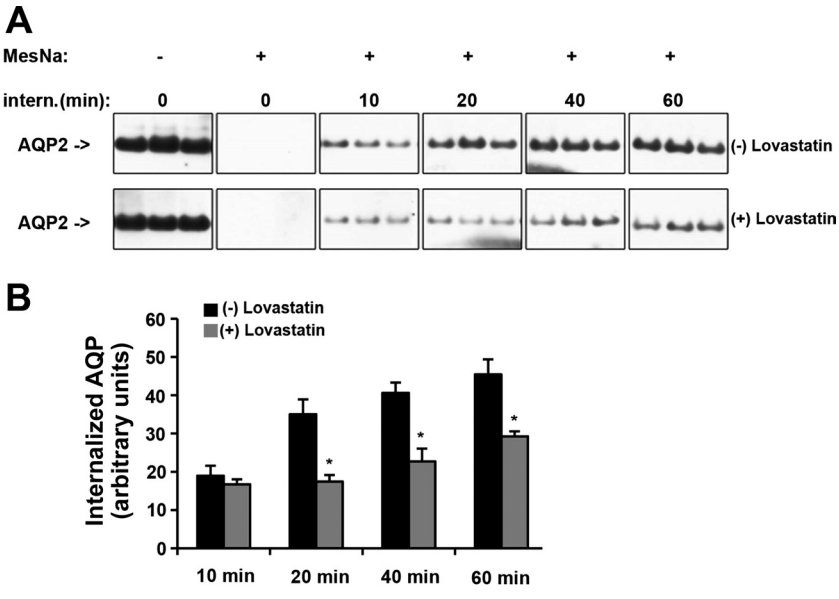

Fig. 7. Internalization assay showing that mild cholesterol depletion inhibits AQP2 endocytosis. *A*: MDC4 cells were either left in control medium (−lovastatin) or in the presence of lovastatin (+lovastatin) for 72 h. Cells were then stimulated with FK for 20 min and biotinylated from the apical side. Subsequently, cells were allowed to internalize biotinylated proteins for the indicated time (intern.). The remaining surface-accessible biotin was stripped with MesNa where indicated (MesNa, +). Biotinylated proteins were recovered and immunoblotted for AQP2. *B*: densitometric analysis of 29-kDa biotinylated AQP2 band. Values are means ± SE of 3 independent experiments. $*P < 0.02$.

and-release experiment described before under normal cholesterol concentrations or after strong cholesterol depletion. Briefly, cells were left in conventional medium or cultured for 72 h in LDL-free medium supplemented with lovastatin and mevalonate before treatment with BFA for 16 h. BFA was washed out, and cells were examined at the conventional time points. AQP2 and AQP4 were visualized at each time point by confocal microscopy, and results are reported in Fig. 8. Colocalization of AQP2 and AQP4 at each time point with markers of the plasma membrane (Na^+-K^+-ATPase), ER (calnexin), and peripheral Golgi (58K protein) is reported in Supplemental Figs. S3 and S4. In MCD4 cell, strong cholesterol depletion resulted in a clear AQP2 accumulation in large perinuclear vesicles compared with the scattered vesicular staining visible under normal cholesterol concentrations (Fig. 8, AQP2, control, +lovastatin). BFA treatment, regardless of endogenous cholesterol levels, induced AQP2 accumulation in the ER (Fig. 8, AQP2, BFA). The export of AQP2 from ER to the Golgi apparatus started 30 min after BFA washout (Fig. 8, AQP2, 30′ WO) and was completed within 1 h 30 min in both experimental conditions (Fig. 8, AQP2, 1h 30′ WO). So far, these results indicated that AQP2 transport from the ER to the Golgi was not affected by cholesterol depletion. Three hours after BFA removal, AQP2 started to proceed from the Golgi to the vesicular storage compartment, as clearly shown in control cells (Fig. 8, AQP2, 3h WO, −lovastatin). At this time, a significant amount of AQP2 entered the post-Golgi vesicular compartment. In contrast, in cholesterol-depleted cells AQP2 was still blocked in the Golgi (Fig. 8, AQP2, 3h WO, +lovastatin), showing that the exit of AQP2 from the Golgi apparatus was delayed under cholesterol depletion. This phenomenon became much more evident 4 h 30 min after BFA washout, when AQP2 was mainly expressed in the vesicular compartment in control cells and still accumulated in the Golgi apparatus in cholesterol-depleted cells (Fig. 8, AQP2, 4h 30′ WO). The detergent insolubility of AQP2 was examined in all the experimental conditions described above and reported in Supplemental Fig. S2. The results clearly show that treatment with lovastatin, by reducing the cholesterol level, significantly increase the amount of soluble AQP2 especially during its transition in the ER and Golgi apparatus.

To demonstrate that cholesterol depletion was not generally affecting the sorting of all proteins, including basolateral ones, we performed the same experiment in M1-AQP4 cells stably expressing AQP4 (Fig. 8, AQP4). In untreated cells, AQP4 was expressed at the basolateral membrane and BFA treatment accumulated AQP4 in the ER. After 30 min of BFA washout, in almost all of the observed cells AQP4 was already transiting the Golgi apparatus. At 1 h 30 min, most of AQP4 was still in the Golgi apparatus while a detectable amount was already delivered to the basolateral plasma membrane. At 3 h, most of the AQP4 was expressed at the plasma membrane and transport was complete at 4 h 30 min. Cholesterol depletion did not affect the transport of newly synthesized AQP4 at any of the time points considered. This finding strongly indicates that AQP2 apical sorting at the Golgi requires the presence of cholesterol, a major component of membrane rafts. Cholesterol depletion clearly retains AQP2 in the Golgi apparatus. This

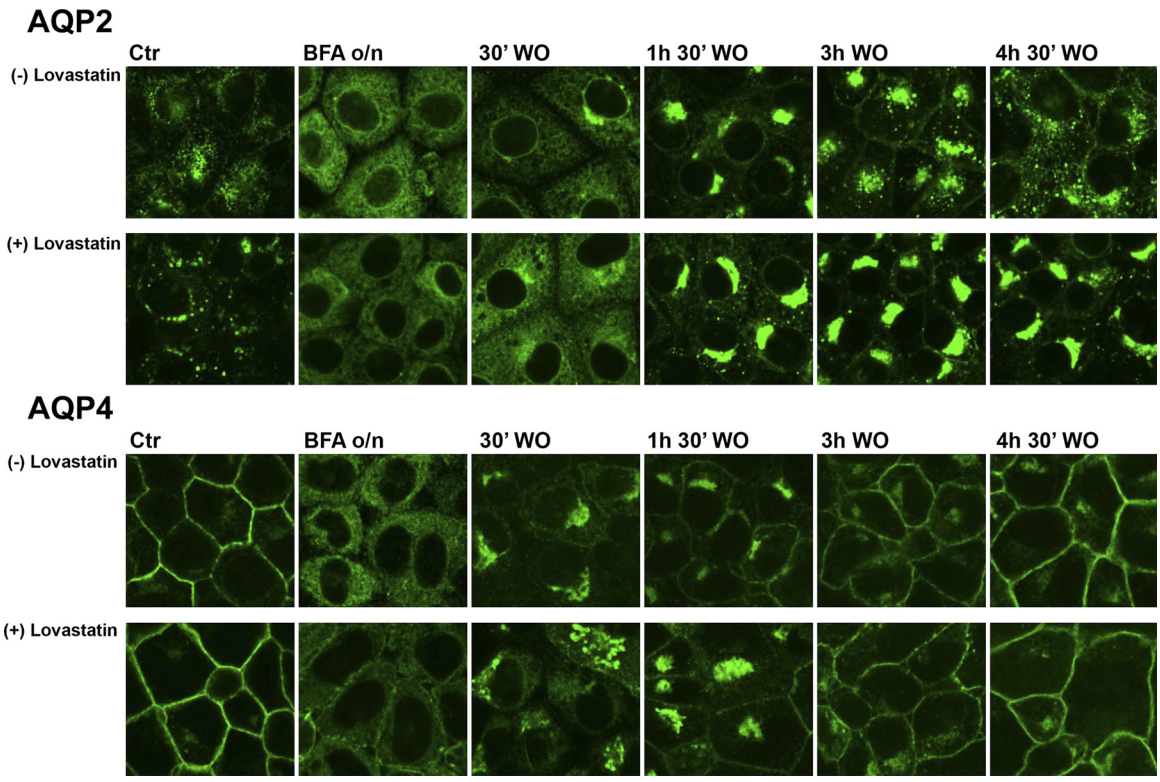

Fig. 8. Block-and-release experiments showing that the exit of AQP2 from TGN is delayed after strong cholesterol depletion. *A*: MDC4 cells (AQP2) and M-1-AQP4 (AQP4) were left either in control medium (−lovastatin) or in the presence of lovastatin in LDL-depleted medium (+lovastatin) for 72 h. Both cell lines were then subjected to block-and-release experiment (see MATERIALS AND METHODS). At each step, the localization of AQP2 and AQP4 was analyzed by immunofluorescence confocal microscopy.

effect was not seen on AQP4 expressed at the basolateral membrane in the same cells.

DISCUSSION

In this work, we provide new evidence that association of the water channel AQP2 with cholesterol/membrane rafts is important for both apical sorting at the TGN and endocytosis from the apical membrane. A number of evidences suggest a role for membrane rafts in AQP2 trafficking. First of all is the presence of AQP2 in the apical microvilli in both native kidney (39, 75) and cell culture models (unpublished observations). It has long been recognized that the microvillar surface of the brush border is organized in cholesterol/sphingolipid-enriched membrane microdomains commonly known as membrane rafts (12). AQP5, expressed in salivary glands, lacrimal glands, and airway epithelium, is also capable of shuttling to and from the apical membrane and, interestingly, its dynamic association with membrane rafts during translocation to the membrane has been demonstrated (29). Recently, Yu et al. (77) have found AQP1, AQP2, and AQP4 in the DRMs from inner medullary collecting duct by tandem liquid chromatography-mass spectrometry.

Membrane rafts have been implicated in the regulation of numerous cellular events, including signal transduction (61) and membrane traffic (27). The large majority of studies on membrane rafts have relied on their detergent insolubility for their effective purification. Enrichment of a protein in DRMs shows that it is raftophilic and is likely to associate with rafts when they form. The most widely used detergent in these studies is Triton X-100, although more recently a wider spectrum of detergents has been utilized to purify rafts and these studies have lead to the suggestion that insolubility in different detergents reflects the association of proteins with distinct types of "raft" domains.

In the present work, we investigated the presence of AQP2 in DRMs extracted with different nonionic detergents, TX-100 and L-WX, from MCD4 cells (28, 49) and rat inner medullary collecting duct. In both cell culture and kidney, AQP2 is more soluble in TX-100 and almost completely insoluble in L-WX. The difference in the solubility of AQP2 in detergents like TX-100 and L-WX, characterized by different hydrophilic-lipophilic balance (HLB), may indicate that *1*) AQP2 is associated with membrane rafts that are better preserved by a milder detergent like L-WX compared with a stronger detergent like TX-100; and *2*) the presence in renal cells of at least two subtype of membrane rafts, one TX insoluble in which AQP2 is only slightly associated, the other, L-WX insoluble, in which AQP2 preferentially associates. Interestingly, AQP2 localization to apical microvilli and its different solubility in TX-100 and L-WX resemble the same features as prominin, a pentaspan protein localized to microvilli at the apical cell surface of MDCK cells (55). Association with Lubrol-resistant rafts has been suggested to facilitate the targeting of prominin specifically to microvilli at the apical cell surface. The authors suggested that insolubility in Lubrol and solubility in Triton X-100 were a consequence of prominin association with a novel lipid raft domain. Subsequent work also implicated Lubrol-resistant rafts in apical targeting in polarized hepatic cells (62). Lubrol rafts were implicated in the direct targeting of proteins to the apical cell surface, whereas Triton-insoluble rafts were shown to function in the indirect (via basolateral cell surface) pathway for apical targeting. As Triton X-100 extraction does not preserve the raft association of a number of proteins (61), the identification of Lubrol as a detergent that can isolate Triton-soluble raft proteins appears to be an important development.

We also report evidence here that, in both MCD4 cells and rat kidney, the association of AQP2 with Lubrol rafts is not modified during the cAMP-induced translocation of AQP2 to the apical membrane. The presence of intracellular AQP2 in membrane rafts suggests an early association of AQP2 with these membrane subdomains during biosynthesis rather than association of AQP2 with membrane rafts at the apical membrane.

Both block-and-release experiments performed in MCD4 cells treated with BFA (Fig. 4) and detergent-solubility assays on purified ER membranes (Fig. 5) indicate that a substantial amount of the ER-associated AQP2 is already markedly Lubrol resistant. This supports our hypothesis of an early association of AQP2 with detergent-resistant domains in the ER. Once exported to the Golgi, AQP2 acquires the full Lubrol insolubility likely because of the association with membrane rafts.

It has long been established that DRMs are not exclusively present at the plasma membrane. Previous studies demonstrated that association of proteins with DRMs occurs as early as the Golgi in the secretory pathway (7, 18, 42). Interestingly, both the early Golgi and the ER are involved in the de novo synthesis of sphingolipids and cholesterol (48, 74). However, although the Golgi contains a considerable amount of these components, the ER is known as the organelle with the lowest sphingolipid and cholesterol content within the secretory pathway (26, 48, 74). For this reason, the ER has been considered as an unlikely place for the existence of lipid raft domains. Nonetheless, there are reports proving the existence of DRMs at the ER in mammalian cells. For example, proteins involved in the synthesis and transfer of the Glycosylphosphatidylinositol (GPI) anchors to GPI-anchored proteins have been observed at DRMs within the ER (44, 60). Additionally, the prion protein PrP has been demonstrated to associate with DRMs as early as the ER within the secretory pathway (42, 58). Finally, DRMs were reported to exist within a substructure of the ER, ER-lipid droplets (22). Hayashi and Su (22) demonstrated that σ-1 receptors of the brain are associated with DRMs of ER-lipid droplets. More recently, it has been reported that the novel transmembrane proteins erlin-1 and erlin-2 are enriched in buoyant DRMs and are residents of the ER, supporting the notion that lipid raft-like domains are present in the ER (6). Collectively, the aforementioned reports provide strong evidence for the existence of lipid raft-like domains in the ER and support our hypothesis of an early association of AQP2 with DRMs in the ER.

This motivated us to investigate a possible role of DRMs/rafts through the AQP2 biosynthetic pathway. Much of the evidence for raft function in cells comes from studies pairing DRM association of key proteins with the effect of cholesterol modulators in disrupting function. Such studies have suggested several important roles for rafts, especially in signal transduction (15, 25, 45) and membrane trafficking (32).

An important finding presented in this paper is that strong cholesterol depletion, achieved in MCD4 cells by lovastatin addition in LDL-deficient culture medium, significantly affects

the sorting of AQP2 from the Golgi/TGN to the FK-sensitive storage compartment. This inhibitory effect was not observed with AQP4, a DRM-associated protein whose basolateral sorting seems to be independent by cholesterol levels.

At the level of the TGN, a sorting process leads to transport containers with different protein and lipid composition. Apical containers are derived from sorting platforms enriched in membrane rafts, whereas basolateral sorting relies on the binding of adaptor proteins to short amino acid sequences present in the cytoplasmic tails of proteins. The presence of multiple hierarchical targeting signals has been demonstrated for a number of transmembrane proteins, for which deletion of a basolateral targeting sequence reveals the existence of a subordinate apical targeting determinant (8, 24, 33). Indeed, although AQP4 is associated with membrane rafts in the kidney, the dominant basolateral sorting signals might drive its membrane localization.

In MCD4 cells, with block-and-release experiments we can easily follow the progression of AQP2 along the major stations of the exocytic pathway (ER, Golgi, storage vesicles) under normal cholesterol concentration or after strong cholesterol depletion. In all the experiments performed, we could not see any significant retention of AQP2 in the ER upon cholesterol depletion. On the contrary, statins treatment, in the absence of exogenous sources of cholesterol, deeply affected the exit of AQP2 from the Golgi apparatus. This effect was also confirmed with another experimental strategy of temperature-dependent block of protein sorting by incubating cells at 20°C for 12 h. When cells returned to 37°C, the export of AQP2 from the Golgi to the FK-sensitive storage compartment was significantly delayed by strong cholesterol depletion (data not shown).

We ruled out the possibility that cholesterol depletion, by modifying the lipid composition of Golgi membranes, was affecting the general sorting of any given protein by analyzing the trafficking of AQP4 in the same experimental conditions. AQP4 is a basolateral water channel expressed in many tissues including the kidney where it is coexpressed, along with AQP2, in the principal cells. Unlike AQP2, AQP4 is not glycosylated and its basolateral sorting is determined by the presence of tyrosine-based and dileucine-like proteinaceous motifs in its COOH terminus (35). Nonetheless, AQP4 is associated with DRMs in MCD4 cells, an observation that has already been made in the rat inner medullary collecting duct (77). The fact that AQP4 sorting to the basolateral membrane is not affected by cholesterol depletion would indicate that *1*) in our experimental condition, cholesterol depletion does not perturb the function of the Golgi complex; and *2*) cholesterol is of importance in the apical sorting of AQP2.

Besides selective apical expression, basolateral membrane expression of AQP2 is often detected in connecting tubule cells and inner medullary collecting duct principal cells, whereas cortical collecting ducts and outer medullary collecting duct principal cells exhibited little basolateral labeling (10, 36, 40, 73). Van Balkom and coworkers (73) suggested that the increased hypertonicity of the renal medulla might be fundamental to the basolateral localization of AQP2 in principal cells in antidiuresis. The authors speculated that hyperosmotic stress might induce an apical-to-basolateral translocation of vesicles and associated membrane proteins (73). In such a scenario, cholesterol would still direct AQP2 to the primary target membrane, the apical, then AQP2 would be transcytosed to the basolateral membrane. Christensen and coworkers (10) proposed that the axial heterogeneity of AQP2 basolateral expression in the kidney strongly suggests that cell-specific mechanisms are involved. In this respect, our cell culture model reproduces the main features of cortical collecting duct principal cells (64), such as the exclusive apical expression of AQP2, and would not be, therefore, a good model for studying the role of cholesterol in basolateral trafficking of AQP2.

Interestingly, another important observation we made was that mild cholesterol depletion, achieved in MCD4 cells by lovastatin addition to the complete culture medium, accumulated a significant amount of AQP2 at the apical membrane. The most likely explanation for this phenomenon is that cholesterol depletion affects AQP2 endocytosis, thus increasing its steady-state abundance at the apical plasma membrane. It is well established that AQP2 constitutively recycles to and from the apical plasma membrane in the absence of a cAMP increase (20) and is endocytosed by clathrin-coated pits (66). This implies that AQP2 can be accumulated at the apical plasma membrane simply by blocking its endocytosis. The result of the endocytosis assay unambiguously demonstrated that this is the case.

Although it has long been believed that clathrin-mediated endocytosis and the internalization of proteins associated with lipid rafts were essentially independent processes (43), there is a growing body of evidence that, in some cases, raft domains and the proteins they contain might actually be internalized through clathrin-mediated endocytosis (9, 11, 21).

Moreover, depletion of cholesterol blocks internalization via both caveolae and clathrin-coated pits (1, 50, 61), suggesting that rafts are incorporated in both types of endocytic structures. In addition, membrane raft components like sphingomyelin and cholesterol have been found in early endocytic organelles and in recycling endosomes in MDCK cells (18). Our data about the association of AQP2 with membrane rafts, although it is known that AQP2 is internalized by a clathrin-dependent pathway (66), further emphasize the fact that association of proteins with lipid rafts and the internalization by clathrin-mediated endocytosis should not necessarily be considered as being mutually exclusive events.

Our results are in agreement with previous observations indicating that treatment with the cholesterol-sequestering agent mβCD accumulates AQP2 at the apical plasma membrane in both isolated kidney tubules and cultured renal cells in a phosphorylation-independent manner (34, 56). Our findings represent a significant advance in the field since we specifically demonstrated that cholesterol depletion affects AQP2 endocytosis. In addition, while the in vivo use of mβCD is limited, due to its potential toxicity and its ability to lyse erythrocytes, statins are approve by the Food and Drug Administration for use in humans with or at risk of cardiovascular disease. Side effects are rare, minor, and generally transient. It has been proposed that statins could promote AQP2 accumulation at the apical plasma membrane through different pathways (5). Our data clearly demonstrated for the first time that statin treatment can inhibit AQP2 endocytosis, thus promoting accumulation at the apical membrane. In conclusion, in this work we provide new insight on the molecular mechanisms regulating the apical sorting and endocytosis of AQP2 and suggest potential appli-

cations of statins in the development of novel treatment for V2R-dependent NDI.

ACKNOWLEDGMENTS

We thank Dr. Michael J. Caplan for critical and helpful suggestions. We also thank Dr. Domenica R. Lasorsa for excellent technical assistance.

GRANTS

This work was supported by grants from Telethon (proposal no. GGP04202 to G. Valenti), Research Program of National Interest (PRIN) projects (20078ZZMZW to M. Svelto and to G. Valenti), Centro di Eccellenza di Genomica in campo Biomedico ed Agrario (CEGBA), and Regional Project 2007 to G. Valenti.

DISCLOSURES

No conflicts of interest are declared by the authors.

REFERENCES

1. **Anderson HA, Chen Y, Norkin LC.** Bound simian virus 40 translocates to caveolin-enriched membrane domains, and its entry is inhibited by drugs that selectively disrupt caveolae. *Mol Biol Cell* 7: 1825–1834, 1996.
2. **Benting JH, Rietveld AG, Simons K.** N-glycans mediate the apical sorting of a GPI-anchored, raft-associated protein in Madin-Darby canine kidney cells. *J Cell Biol* 146: 313–320, 1999.
3. **Bichet DG.** Nephrogenic diabetes insipidus. *Adv Chronic Kidney Dis* 13: 96–104, 2006.
4. **Bichet DG.** Vasopressin receptor mutations in nephrogenic diabetes insipidus. *Semin Nephrol* 28: 245–251, 2008.
5. **Bouley R, Hasler U, Lu HA, Nunes P, Brown D.** Bypassing vasopressin receptor signaling pathways in nephrogenic diabetes insipidus. *Semin Nephrol* 28: 266–278, 2008.
6. **Browman DT, Resek ME, Zajchowski LD, Robbins SM.** Erlin-1 and erlin-2 are novel members of the prohibitin family of proteins that define lipid-raft-like domains of the ER. *J Cell Sci* 119: 3149–3160, 2006.
7. **Brown DA, Rose JK.** Sorting of GPI-anchored proteins to glycolipid-enriched membrane subdomains during transport to the apical cell surface. *Cell* 68: 533–544, 1992.
8. **Carmosino M, Gimenez I, Caplan M, Forbush B.** Exon loss accounts for differential sorting of Na-K-Cl cotransporters in polarized epithelial cells. *Mol Biol Cell* 19: 4341–4351, 2008.
9. **Cheng PC, Dykstra ML, Mitchell RN, Pierce SK.** A role for lipid rafts in B cell antigen receptor signaling and antigen targeting. *J Exp Med* 190: 1549–1560, 1999.
10. **Christensen BM, Wang W, Frokiaer J, Nielsen S.** Axial heterogeneity in basolateral AQP2 localization in rat kidney: effect of vasopressin. *Am J Physiol Renal Physiol* 284: F701–F717, 2003.
11. **Cuitino L, Matute R, Retamal C, Bu G, Inestrosa NC, Marzolo MP.** ApoER2 is endocytosed by a clathrin-mediated process involving the adaptor protein Dab2 independent of its rafts' association. *Traffic* 6: 820–838, 2005.
12. **Danielsen EM, Hansen GH.** Lipid rafts in epithelial brush borders: atypical membrane microdomains with specialized functions. *Biochim Biophys Acta* 1617: 1–9, 2003.
13. **Deen PM.** Mouse models for congenital nephrogenic diabetes insipidus: what can we learn from them? *Nephrol Dial Transplant* 22: 1023–1026, 2007.
14. **Deen PM, Van Balkom BW, Savelkoul PJ, Kamsteeg EJ, Van Raak M, Jennings ML, Muth TR, Rajendran V, Caplan MJ.** Aquaporin-2: COOH terminus is necessary but not sufficient for routing to the apical membrane. *Am J Physiol Renal Physiol* 282: F330–F340, 2002.
15. **Dykstra M, Cherukuri A, Sohn HW, Tzeng SJ, Pierce SK.** Location is everything: lipid rafts and immune cell signaling. *Annu Rev Immunol* 21: 457–481, 2003.
16. **Fejes-Toth G, Naray-Fejes-Toth A.** Differentiation of renal beta-intercalated cells to alpha-intercalated and principal cells in culture. *Proc Natl Acad Sci USA* 89: 5487–5491, 1992.
17. **Fey EG, Wan KM, Penman S.** Epithelial cytoskeletal framework and nuclear matrix-intermediate filament scaffold: three-dimensional organization and protein composition. *J Cell Biol* 98: 1973–1984, 1984.
18. **Fra AM, Williamson E, Simons K, Parton RG.** Detergent-insoluble glycolipid microdomains in lymphocytes in the absence of caveolae. *J Biol Chem* 269: 30745–30748, 1994.
19. **Fushimi K, Sasaki S, Marumo F.** Phosphorylation of serine 256 is required for cAMP-dependent regulatory exocytosis of the aquaporin-2 water channel. *J Biol Chem* 272: 14800–14804, 1997.
20. **Gustafson CE, Katsura T, McKee M, Bouley R, Casanova JE, Brown D.** Recycling of AQP2 occurs through a temperature- and bafilomycin-sensitive *trans*-Golgi-associated compartment. *Am J Physiol Renal Physiol* 278: F317–F326, 2000.
21. **Hansen GH, Dalskov SM, Rasmussen CR, Immerdal L, Niels-Christiansen LL, Danielsen EM.** Cholera toxin entry into pig enterocytes occurs via a lipid raft- and clathrin-dependent mechanism. *Biochemistry* 44: 873–882, 2005.
22. **Hayashi T, Su TP.** Sigma-1 receptors (sigma(1) binding sites) form raft-like microdomains and target lipid droplets on the endoplasmic reticulum: roles in endoplasmic reticulum lipid compartmentalization and export. *J Pharmacol Exp Ther* 306: 718–725, 2003.
23. **Hendriks G, Koudijs M, van Balkom BW, Oorschot V, Klumperman J, Deen PM, van der Sluijs P.** Glycosylation is important for cell surface expression of the water channel aquaporin-2 but is not essential for tetramerization in the endoplasmic reticulum. *J Biol Chem* 279: 2975–2983, 2004.
24. **Hobert M, Carlin C.** Cytoplasmic juxtamembrane domain of the human EGF receptor is required for basolateral localization in MDCK cells. *J Cell Physiol* 162: 434–446, 1995.
25. **Holowka D, Gosse JA, Hammond AT, Han X, Sengupta P, Smith NL, Wagenknecht-Wiesner A, Wu M, Young RM, Baird B.** Lipid segregation and IgE receptor signaling: a decade of progress. *Biochim Biophys Acta* 1746: 252–259, 2005.
26. **Holthuis JC, Pomorski T, Raggers RJ, Sprong H, Van Meer G.** The organizing potential of sphingolipids in intracellular membrane transport. *Physiol Rev* 81: 1689–1723, 2001.
27. **Ikonen E.** Roles of lipid rafts in membrane transport. *Curr Opin Cell Biol* 13: 470–477, 2001.
28. **Iolascon A, Aglio V, Tamma G, D'Apolito M, Addabbo F, Procino G, Simonetti MC, Montini G, Gesualdo L, Debler EW, Svelto M, Valenti G.** Characterization of two novel missense mutations in the AQP2 gene causing nephrogenic diabetes insipidus. *Nephron Physiol* 105: p33–p41, 2007.
29. **Ishikawa Y, Yuan Z, Inoue N, Skowronski MT, Nakae Y, Shono M, Cho G, Yasui M, Agre P, Nielsen S.** Identification of AQP5 in lipid rafts and its translocation to apical membranes by activation of M3 mAChRs in interlobular ducts of rat parotid gland. *Am J Physiol Cell Physiol* 289: C1303–C1311, 2005.
30. **Kamsteeg EJ, Hendriks G, Boone M, Konings IB, Oorschot V, van der Sluijs P, Klumperman J, Deen PM.** Short-chain ubiquitination mediates the regulated endocytosis of the aquaporin-2 water channel. *Proc Natl Acad Sci USA* 103: 18344–18349, 2006.
31. **Keller P, Simons K.** Cholesterol is required for surface transport of influenza virus hemagglutinin. *J Cell Biol* 140: 1357–1367, 1998.
32. **Kirkham M, Parton RG.** Clathrin-independent endocytosis: new insights into caveolae and non-caveolar lipid raft carriers. *Biochim Biophys Acta* 1746: 349–363, 2005.
33. **Koivisto UM, Hubbard AL, Mellman I.** A novel cellular phenotype for familial hypercholesterolemia due to a defect in polarized targeting of LDL receptor. *Cell* 105: 575–585, 2001.
34. **Lu H, Sun TX, Bouley R, Blackburn K, McLaughlin M, Brown D.** Inhibition of endocytosis causes phosphorylation (S256)-independent plasma membrane accumulation of AQP2. *Am J Physiol Renal Physiol* 286: F233–F243, 2004.
35. **Madrid R, Le Maout S, Barrault MB, Janvier K, Benichou S, Merot J.** Polarized trafficking and surface expression of the AQP4 water channel are coordinated by serial and regulated interactions with different clathrin-adaptor complexes. *EMBO J* 20: 7008–7021, 2001.
36. **Marples D, Knepper MA, Christensen EI, Nielsen S.** Redistribution of aquaporin-2 water channels induced by vasopressin in rat kidney inner medullary collecting duct. *Am J Physiol Cell Physiol* 269: C655–C664, 1995.
37. **Matter K.** Epithelial polarity: sorting out the sorters. *Curr Biol* 10: R39–42, 2000.
38. **Nedvetsky PI, Tamma G, Beulshausen S, Valenti G, Rosenthal W, Klussmann E.** Regulation of aquaporin-2 trafficking. *Handb Exp Pharmacol*: 133–157, 2009.
39. **Nielsen S, Chou CL, Marples D, Christensen EI, Kishore BK, Knepper MA.** Vasopressin increases water permeability of kidney collecting

duct by inducing translocation of aquaporin-CD water channels to plasma membrane. *Proc Natl Acad Sci USA* 92: 1013–1017, 1995.
40. **Nielsen S, DiGiovanni SR, Christensen EI, Knepper MA, Harris HW.** Cellular and subcellular immunolocalization of vasopressin-regulated water channel in rat kidney. *Proc Natl Acad Sci USA* 90: 11663–11667, 1993.
41. **Noda Y, Horikawa S, Kanda E, Yamashita M, Meng H, Eto K, Li Y, Kuwahara M, Hirai K, Pack C, Kinjo M, Okabe S, Sasaki S.** Reciprocal interaction with G-actin and tropomyosin is essential for aquaporin-2 trafficking. *J Cell Biol* 182: 587–601, 2008.
42. **Paladino S, Sarnataro D, Pillich R, Tivodar S, Nitsch L, Zurzolo C.** Protein oligomerization modulates raft partitioning and apical sorting of GPI-anchored proteins. *J Cell Biol* 167: 699–709, 2004.
43. **Parton RG, Richards AA.** Lipid rafts and caveolae as portals for endocytosis: new insights and common mechanisms. *Traffic* 4: 724–738, 2003.
44. **Pielsticker LK, Mann KJ, Lin WL, Sevlever D.** Raft-like membrane domains contain enzymatic activities involved in the synthesis of mammalian glycosylphosphatidylinositol anchor intermediates. *Biochem Biophys Res Commun* 330: 163–171, 2005.
45. **Pike LJ.** Lipid rafts: bringing order to chaos. *J Lipid Res* 44: 655–667, 2003.
46. **Pitas RE, Innerarity TL, Weinstein JN, Mahley RW.** Acetoacetylated lipoproteins used to distinguish fibroblasts from macrophages in vitro by fluorescence microscopy. *Arteriosclerosis* 1: 177–185, 1981.
47. **Poole K, Meder D, Simons K, Muller D.** The effect of raft lipid depletion on microvilli formation in MDCK cells, visualized by atomic force microscopy. *FEBS Lett* 565: 53–58, 2004.
48. **Prinz W.** Cholesterol trafficking in the secretory and endocytic systems. *Semin Cell Dev Biol* 13: 197–203, 2002.
49. **Procino G, Barbieri C, Tamma G, De Benedictis L, Pessin JE, Svelto M, Valenti G.** AQP2 exocytosis in the renal collecting duct—involvement of SNARE isoforms and the regulatory role of Munc18b. *J Cell Sci* 121: 2097–2106, 2008.
50. **Procino G, Carmosino M, Marin O, Brunati AM, Contri A, Pinna LA, Mannucci R, Nielsen S, Kwon TH, Svelto M, Valenti G.** Ser-256 phosphorylation dynamics of aquaporin 2 during maturation from the ER to the vesicular compartment in renal cells. *FASEB J* 17: 1886–1888, 2003.
51. **Raunser S, Haase W, Franke C, Eckert GP, Muller WE, Kuhlbrandt W.** Heterologously expressed GLT-1 associates in approximately 200-nm protein-lipid islands. *Biophys J* 91: 3718–3726, 2006.
52. **Ridsdale A, Denis M, Gougeon PY, Ngsee JK, Presley JF, Zha X.** Cholesterol is required for efficient endoplasmic reticulum-to-Golgi transport of secretory membrane proteins. *Mol Biol Cell* 17: 1593–1605, 2006.
53. **Rodal SK, Skretting G, Garred O, Vilhardt F, van Deurs B, Sandvig K.** Extraction of cholesterol with methyl-beta-cyclodextrin perturbs formation of clathrin-coated endocytic vesicles. *Mol Biol Cell* 10: 961–974, 1999.
54. **Rodriguez-Boulan E, Gonzalez A.** Glycans in post-Golgi apical targeting: sorting signals or structural props? *Trends Cell Biol* 9: 291–294, 1999.
55. **Roper K, Corbeil D, Huttner WB.** Retention of prominin in microvilli reveals distinct cholesterol-based lipid micro-domains in the apical plasma membrane. *Nat Cell Biol* 2: 582–592, 2000.
56. **Russo LM, McKee M, Brown D.** Methyl-β-cyclodextrin induces vasopressin-independent apical accumulation of aquaporin-2 in the isolated, perfused rat kidney. *Am J Physiol Renal Physiol* 291: F246–F253, 2006.
57. **Sands JM, Bichet DG.** Nephrogenic diabetes insipidus. *Ann Intern Med* 144: 186–194, 2006.
58. **Sarnataro D, Campana V, Paladino S, Stornaiuolo M, Nitsch L, Zurzolo C.** PrP(C) association with lipid rafts in the early secretory pathway stabilizes its cellular conformation. *Mol Biol Cell* 15: 4031–4042, 2004.
59. **Sasaki M, Ishikawa SE.** Renal action of vasopressin. *Nippon Rinsho* 64, Suppl 2: 257–264, 2006.
60. **Sevlever D, Pickett S, Mann KJ, Sambamurti K, Medof ME, Rosenberry TL.** Glycosylphosphatidylinositol-anchor intermediates associate with triton-insoluble membranes in subcellular compartments that include the endoplasmic reticulum. *Biochem J* 343: 627–635, 1999.
61. **Simons K, Toomre D.** Lipid rafts and signal transduction. *Nat Rev Mol Cell Biol* 1: 31–39, 2000.
62. **Slimane TA, Trugnan G, Van ISC, Hoekstra D.** Raft-mediated trafficking of apical resident proteins occurs in both direct and transcytotic pathways in polarized hepatic cells: role of distinct lipid microdomains. *Mol Biol Cell* 14: 611–624, 2003.
63. **Song KS, Li S, Okamoto T, Quilliam LA, Sargiacomo M, Lisanti MP.** Co-purification and direct interaction of Ras with caveolin, an integral membrane protein of caveolae microdomains. Detergent-free purification of caveolae microdomains. *J Biol Chem* 271: 9690–9697, 1996.
64. **Stoos BA, Naray-Fejes-Toth A, Carretero OA, Ito S, Fejes-Toth G.** Characterization of a mouse cortical collecting duct cell line. *Kidney Int* 39: 1168–1175, 1991.
65. **Subtil A, Gaidarov I, Kobylarz K, Lampson MA, Keen JH, McGraw TE.** Acute cholesterol depletion inhibits clathrin-coated pit budding. *Proc Natl Acad Sci USA* 96: 6775–6780, 1999.
66. **Sun TX, Van Hoek A, Huang Y, Bouley R, McLaughlin M, Brown D.** Aquaporin-2 localization in clathrin-coated pits: inhibition of endocytosis by dominant-negative dynamin. *Am J Physiol Renal Physiol* 282: F998–F1011, 2002.
67. **Takata K.** Aquaporin-2 (AQP2): its intracellular compartment and trafficking. *Cell Mol Biol (Noisy-le-grand)* 52: 34–39, 2006.
68. **Takata K, Matsuzaki T, Tajika Y, Ablimit A, Hasegawa T.** Localization and trafficking of aquaporin 2 in the kidney. *Histochem Cell Biol* 130: 197–209, 2008.
69. **Tamma G, Procino G, Strafino A, Bononi E, Meyer G, Paulmichl M, Formoso V, Svelto M, Valenti G.** Hypotonicity induces aquaporin-2 internalization and cytosol-to-membrane translocation of ICln in renal cells. *Endocrinology* 148: 1118–1130, 2007.
70. **Terris J, Ecelbarger CA, Marples D, Knepper MA, Nielsen S.** Distribution of aquaporin-4 water channel expression within rat kidney. *Am J Physiol Renal Fluid Electrolyte Physiol* 269: F775–F785, 1995.
71. **Valenti G, Procino G, Tamma G, Carmosino M, Svelto M.** Minireview: aquaporin 2 trafficking. *Endocrinology* 146: 5063–5070, 2005.
72. **van Balkom BW, Graat MP, van Raak M, Hofman E, van der Sluijs P, Deen PM.** Role of cytoplasmic termini in sorting and shuttling of the aquaporin-2 water channel. *Am J Physiol Cell Physiol* 286: C372–C379, 2004.
73. **van Balkom BW, van Raak M, Breton S, Pastor-Soler N, Bouley R, van der Sluijs P, Brown D, Deen PM.** Hypertonicity is involved in redirecting the aquaporin-2 water channel into the basolateral, instead of the apical, plasma membrane of renal epithelial cells. *J Biol Chem* 278: 1101–1107, 2003.
74. **van Meer G, Lisman Q.** Sphingolipid transport: rafts and translocators. *J Biol Chem* 277: 25855–25858, 2002.
75. **Yamamoto T, Sasaki S, Fushimi K, Ishibashi K, Yaoita E, Kawasaki K, Marumo F, Kihara I.** Vasopressin increases AQP-CD water channel in apical membrane of collecting duct cells in Brattleboro rats. *Am J Physiol Cell Physiol* 268: C1546–C1551, 1995.
76. **Yamashita Y, Hirai K, Katayama Y, Fushimi K, Sasaki S, Marumo F.** Mutations in sixth transmembrane domain of AQP2 inhibit its translocation induced by vasopressin. *Am J Physiol Renal Physiol* 278: F395–F405, 2000.
77. **Yu MJ, Pisitkun T, Wang G, Aranda JF, Gonzales PA, Tchapyjnikov D, Shen RF, Alonso MA, Knepper MA.** Large-scale quantitative LC-MS/MS analysis of detergent-resistant membrane proteins from rat renal collecting duct. *Am J Physiol Cell Physiol* 295: C661–C678, 2008.